Theory of the upper critical field in anisotropic superconductors

Daniel W. Youngner and Richard A. Klemm
Ames Laboratory— U.S. Department of Energy and Department of Physics, Iowa State University, Ames, Iowa 50011
(Received 20 August 1979)

The upper critical field in superconductors is calculated using a model which incorporates anisotropy in both the Fermi surface and the superconducting pair state. The effects of nonlocality are included to all orders in perturbation theory, giving results valid over nearly the entire temperature range. It is shown that increasing Fermi-surface anisotropy causes H_{c2} to become more nearly linear in temperature, whereas even small amounts of pair-state anisotropy cause positive curvature in $H_{c2}(T)$ near T_{c0}. All effects of anisotropy are diminished by increasing the impurity scattering rate. The theory is fit to experimental data on $NbSe_2$.

I. INTRODUCTION

The upper critical fields of materials with anisotropic Fermi surfaces have been the subject of many recent experimental investigations.[1–7] In some of the anisotropic materials the $H_{c2}(T)$ curve displays positive curvature near T_{c0} and retains anomolously high values as T approaches zero. Recent experimental work by Orlando *et al.*,[1] for example, shows upward curvature in the critical-field curve of the A-15 material Nb_3Sn, and perpendicular field measurements made by Dalrymple and Prober[2] and others[3,4] on the hexagonally distorted material $NbSe_2$ show H_{c2} exceeding the predicted[8] value for spherically symmetric materials by $\sim 20\%$ in the low-temperature regime. Similar effects are seen in other[5–7] anisotropic materials.

Theoretical models describing these features should include nonlocality of the superconducting pair state as well as anisotropy in both the Fermi surface and the pair state. Several years ago Helfand and Werthamer[8] showed how to treat nonlocality in isotropic materials exactly. A short time later, Hohenberg and Werthamer[9] did a quasilocal calculation demonstrating that Fermi-surface anisotropy can cause upward curvature in $H_{c2}(T)$ near T_{c0}. Takanaka and Nagashima[10] (TN) extended the work of Hohenberg and Werthamer by retaining higher-order terms in the nonlocality and by perturbatively introducing gap anisotropy. The applicability of their (TN) work is limited to the immediate vicinity of T_{c0}. Teichler,[11] using a different formalism, found expressions for the first few terms in a cubic harmonic series expansion of the contributions to $H_{c2}(T)$ from anisotropy in the Fermi velocity and the electron-electron coupling. He obtained results for all temperatures, but predicted that $H_{c2}(T)$ could deviate either above or below the Helfand and Werthamer[8] curve depending on the phases of the anisotropies of the Fermi velocity and the e-e coupling. (No anisotropy-induced reduction of the Helfand-Werthamer curve has ever been seen experimentally.)

In this paper we extend the Hohenberg-Werthamer[9] theory of the upper critical field by summing to infinite order the effects of nonlocality, and by perturbatively including Fermi surface and pair-state anisotropy. We will restrict our consideration to fields applied along crystal symmetry axes, and will concern ourselves primarily with clean materials since it is in them that the effects of anisotropy are most pronounced.

In Sec. II we formulate the theory. In Sec. III we describe the theory appropriate for materials with general Fermi-surface anisotropy but unperturbed pair states. In Sec. IV we allow both the Fermi surface and the pair state to be anisotropic and fit experimental upper critical field data on $NbSe_2$ in the perpendicular field direction.

II. DESCRIPTION OF THE THEORY

The foundations for our theory are described by Hohenberg and Werthamer[9] and references therein. The assumptions made were that the transition to the superconducting state is second order (only terms linear in the gap in the Gor'kov equation are retained), the electron-electron coupling is isotropic and weak, the electron scattering centers are randomly located and nonmagnetic, and the effect of the magnetic field on the orbital motion of the electrons may be treated in the semiclassical approximation.[12] The Fermi surface may contain only one band. Although Hohenberg and Werthamer considered only the case for which the Fermi-surface anisotropy was small and the pair state was isotropic, the formalism they developed is sufficiently general as to allow arbitrary shapes for both the Fermi surface and the pair

state. We begin with Eqs. (5) and (11) from Ref. 9, the solution of which gives $H_{c2}(T)$:

$$1 = gN(0)T \sum_{\nu=-\infty}^{\infty} (S_\omega^{-1} - 1/2\tau)^{-1} \ , \tag{1}$$

where

$$S_\omega = \frac{\pi}{|\tilde{\omega}|} \int d\hat{q} N(\hat{q}) \sum_{n=0}^{\infty} (-1)^n \left\langle S \left| \left(\frac{\vec{v}\cdot\vec{\pi}}{2\tilde{\omega}} \right)^{2n} \right| S \right\rangle \ . \tag{2}$$

In Eqs. (1) and (2) g, $N(0)$, $1/\tau(\equiv n|u|^2)$, $N(\hat{q})$, and $\vec{v}$ are, respectively, the BCS coupling constant, the average density of states at the Fermi surface, the electron scattering rate (or the product of the impurity concentration and the square of the impurity scattering amplitude), the density of states at the Fermi surface in direction $\hat{q}$, and the Fermi velocity. Furthermore, $\vec{\pi} \equiv -i\vec{\nabla} - 2e\vec{A}$ is the gauge-invariant momentum operator acting on the pair state $|S\rangle$ (described more fully later), and $\tilde{\omega} \equiv \omega_\nu + \mathrm{sgn} \times (\omega_\nu/2\tau)$ is the Matsubara frequency renormalized by impurities. As usual, τ is the impurity scattering time, $\omega_\nu = (2\nu+1)\pi T$ (ν = integer), $e = |e|$, and $\vec{A}$ is the magnetic vector potential. We remark that S_ω is the nonlocal pair propagator in the ladder approximation for the scattering, and Eq. (1) includes the usual vertex renormalization. Anticipating isomorphism with the harmonic-oscillator problem,[8,13] we choose $\vec{H} = (0, 0, -H)$, and $\vec{A} = (0, -Hx, 0)$ where the $\hat{z}$ axis may be any one of the three crystal axes. Units have been chosen such that $\hbar = k_B = c = 1$.

By inserting $1/|2\nu+1| - 1/|2\nu+1|$ in the ν sum in Eq. (2) and introducing the Debye frequency cutoff in the first of these sums in the usual manner, Eq. (1) becomes

$$\ln \frac{T}{T_{c0}} = \sum_{\nu=-\infty}^{\infty} \left[T\left(S_\omega^{-1} - \frac{1}{2\tau} \right)^{-1} - \frac{1}{|2\nu+1|} \right] \ , \tag{3}$$

where $T_{c0} = (2\gamma\omega_D)/\pi \exp[-1/gN(0)]$ is the zero-field transition temperature, $\gamma = 1.781$ is the exponential of Euler's constant, and ω_D is the Debye frequency.

The equations we have written so far are formally identical to those in Ref. 9. We will extend their scope by deriving expressions for S_ω which are valid for all temperatures and for arbitrarily shaped single-band Fermi surfaces (Sec. III), and by considering the modifications to S_ω resulting from the inclusion of anisotropy in the superconducting pair state (Sec. IV).

III. ANISOTROPIC FERMI SURFACE

The nonlocal contributions to S_ω for materials with distorted Fermi surfaces but undistorted pair states can be summed analytically to infinite order. Following Helfand and Werthamer[8] we initially take the pair state $|S\rangle$ to be the lowest eigenstate of the harmonic-oscillator operator $\pi^2/2m$. We denote this lowest state by $|0\rangle$. In real space, the wave function of this state is

$$\Delta_0(\vec{r}) = \langle \vec{r}|0\rangle = \exp(-eH_{c2}x^2) \ .$$

The system is quantized by setting $\pi_-|0\rangle = 0$ where $\pi_\pm = \pi_x \pm i\pi_y$, and establishing the commutation relations

$$[\pi_+, \pi_z] = [\pi_-, \pi_z] = 0 \ , \quad [\pi_-, \pi_+] = 4eH_{c2} \equiv \epsilon \ .$$

For fields applied along crystal symmetry axes we expect the pair state to have no momentum parallel to the field, so $\pi_z|0\rangle = 0$.

The expectation values from Eq. (2) of the form $\langle 0|(\vec{v}\cdot\vec{\pi})^{2n}|0\rangle$ can be determined by establishing a recursion relation. It is easy to show that

$$\langle 0|(\vec{v}\cdot\vec{\pi})^2|0\rangle = v_+v_-\epsilon \equiv v_\perp^2 eH_{c2} \ , \tag{4}$$

$$[v_\pm = \tfrac{1}{2}(v_x \pm iv_y)] \ .$$

Furthermore,

$$\langle 0|(\vec{v}\cdot\vec{\pi})^{2n+2}|0\rangle = (2n+1)v_+v_-\epsilon \langle 0|(\vec{v}\cdot\vec{\pi})^{2n}|0\rangle \tag{5}$$

so by induction

$$\langle 0|(\vec{v}\cdot\vec{\pi})^{2n}|0\rangle = (v_+v_-)^n\epsilon^n(2n-1)!! \ , \tag{6a}$$

$$= (v_\perp^2 eH_{c2})^n(2n-1)!! \ . \tag{6b}$$

The sum in Eq. (2) then becomes

$$\sum_{n=0}^{\infty} (-1)^n \left\langle 0 \left| \left(\frac{\vec{v}\cdot\vec{\pi}}{2\tilde{\omega}} \right)^{2n} \right| 0 \right\rangle = 1 + \sum_{n=1}^{\infty} (-1)^n a^n (2n-1)!! \tag{7}$$

$$= \sqrt{\pi} z \exp(z^2) \operatorname{erfc}(z) \ , \tag{8}$$

where $z = (2a)^{-1/2}$, $a = v_\perp^2 eH_{c2}/4\tilde{\omega}^2$, and $\operatorname{erfc}(z)$ is the complimentary error function.

Notice that the perturbation series [Eq. (7)] treating the effects of nonlocality is asymptotic. If one attempts to evaluate it by retaining increasingly higher-order terms[14] he finds that his approximation to $H_{c2}(T)$ improves in an increasingly narrow neighborhood of T_{c0}, but diverges at increasingly higher temperatures. To obtain results valid over the entire temperature range, this series must be summed to infinite order [Eq. (8)].

When Eq. (8) is substituted into Eq. (2) we have an integral over the Fermi surface which must in general be evaluated numerically. This is done by picking a particular ν value and evaluating the exact form of the n sum [Eq. (8)] for each of a dense series of points on the Fermi surface. This procedure is repeated for enough ν values that the ν sum is evaluated reliably. When $\lambda \equiv 1/(2\pi T_{c0}\tau) \neq 0$, H_{c2}

TABLE I. Slopes ($-dh/dt \pm 0.2\%$) at $t=1$ of the curves in Figs. 1 and 3–7.

	Curve				
	1	2	3	4	5
Fig.					
1	0.711	1.055	3.70	31.8	
3	0.711	0.722	0.749	0.781	0.829
4	0.781	1.151	4.32	34.6	
5	0.781	0.627	0.405		
6	0.627	0.627	0.627		
7	0.781	0.669	0.672	0.627	

and T are first estimated then determined self-consistently. Numerical solutions to Eqs. (2) and (3) assuming a spherical Fermi surface and various values of λ are shown in Fig. 1. Here $t \equiv T/T_{c0}$, $h \equiv eH_{c2}v_F^2/(2\pi T_{c0})^2$, and $h^*(t) \equiv h(t)/(-dh/dt|_{t=1})$. These solutions are numerically identical to those in Ref. 8 and are included here for future comparisons. [In Appendix A we show analytically that when the Fermi surface is spherical and $\lambda=0$, our more general equations defining $H_{c2}(T)$ reduce to those of Helfand and Werthamer.] The slopes of all curves in Figs. 1 and 3–7 have been fixed to be -1 at $t=1$. Table I contains the actual slopes at $t=1$ for each of these curves.

Fermi-surface anisotropy enters the calculations through the quantities $N(\hat{q})$ and $v_1^{2n}(\hat{q})$. For materials with hexagonally symmetric distortions (such as the transition-metal dichalcogenides with the field perpendicular to the layers) we model the Fermi surface by setting

$$|v_\perp(\hat{q})| = v_F[1+b_6(6\phi)]\cdot\sin\theta$$

and $N(\hat{q}) \sim 1/|v(\hat{q})|$, where θ and ϕ are the polar and azimuthal angles, respectively. Figure 2 shows how cross sections of the Fermi surface would appear for $b_6=0.0$, 0.15, 0.3, and Fig. 3 shows the upper critical field curves for materials with hexagonally distorted Fermi surfaces. We observe that increasing Fermi-surface anisotropy causes the $h^*(t)$ curve to lie increasingly above the Helfand-Werthamer curve; for $b_6=0.5$ the upper critical field is nearly linear in temperature. Although we have plotted results only for hexagonally symmetric Fermi surfaces, identical results are obtained with $v_\perp(\hat{q}) = v_F\sin\theta \times(1+b\cos n\phi)$ for all n. We therefore conclude that it is the magnitude and not the shape of the Fermi-surface anisotropy that determines the enhancement of $H_{c2}(T)$.

Since impurity scattering tends to smear out the Fermi surface, we expect that increasing impurity scattering should drive the $H_{c2}(T)$ curves towards the isotropic dirty limit curve of Helfand and Werthamer. Figure 4 shows the results of numerical calculations

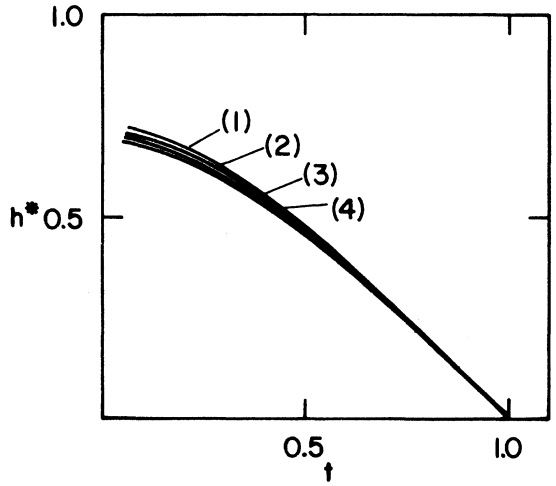

FIG. 1. Upper critical fields for spherically symmetric materials. $\lambda=$(1) 0.0; (2) 0.5; (3) 5.0; (4) 50.0.

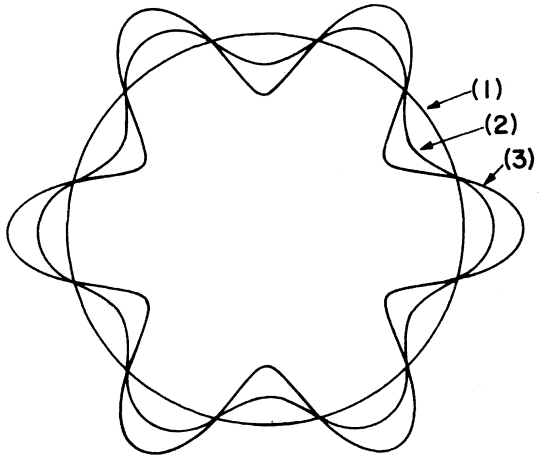

FIG. 2. Cross-sectional shapes of the Fermi surface. $b_6=$(1) 0.0; (2) 0.15; (3) 0.3.

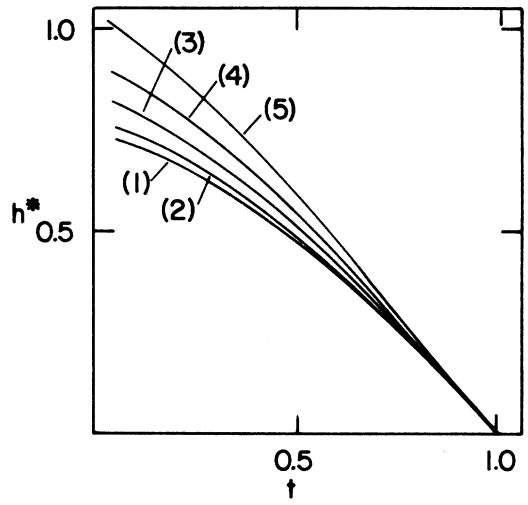

FIG. 3. Upper critical fields for materials with distorted Fermi surfaces. $\lambda=0.0$, $b_6=(1)$ 0.0; (2) 0.15; (3) 0.3; (4) 0.4; (5) 0.5.

with $b=0.4$ and $\lambda=0.0$, 0.5, 5.0, and $50.0\approx\infty$. (When $\lambda=1.0$, the electron scattering length is roughly equal to the pair coherence length.) We note that the $\lambda=50.0$ curve is essentially identical to the isotropic dirty limit curve of Helfand and Werthamer. However, for $\lambda=5$, which describes relatively dirty materials, $h^*(t)$ for $b=0.4$ still lies above the isotropic clean limit curve. A material must be quite dirty before the effects of Fermi-surface anisotropy vanish completely.

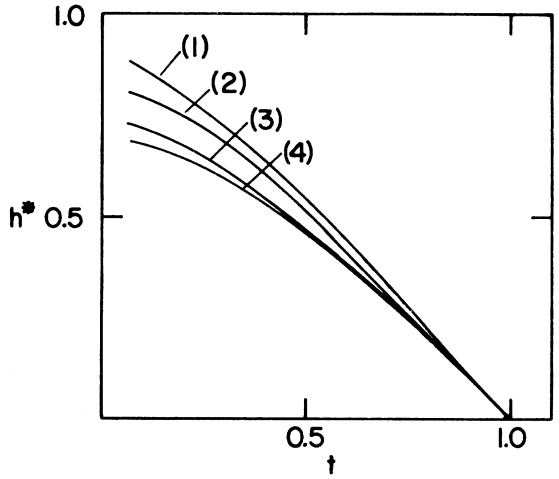

FIG. 4. Upper critical fields for materials with distorted Fermi surfaces and impurity scattering. $b_6=0.4$, $\lambda=(1)$ 0.0; (2) 0.5; (3) 5.0; (4) 50.0.

IV. ANISOTROPIC PAIR STATES

It is expected that the anisotropy in the superconducting pair state will be strongly dependent on the anisotropy in the Fermi surface as well as on impurity scattering, temperature, and perhaps even the field. Takanaka and Nagashima[10] devised a scheme for relating the pair state anisotropy parameters a_{2n} to the Fermi-surface parameters, but their scheme relied on the assumption that the upper critical field satisfied $\partial H_{c2}/\partial a_{2n}^*=0$. (We know of no physical motivation for making this assumption. It does not necessarily imply that the free energy will be a minimum.) Their resulting expressions for a_2 and a_4 diverged at low temperatures and are therefore unacceptable. In our model the pair-state anisotropy parameters are considered to be free and independent of the Fermi surface, but in practice are always taken to be smaller than the analogous Fermi-surface anisotropy parameters.

In a manner similar to that proposed by Takanaka and Nagashima[10] we write the perturbed pair state as

$$|S\rangle=\left(1+\sum_{m=1}^{\infty}|a_{2m}|^2\right)^{-1/2}\left(1+\sum_{m=1}^{\infty}\frac{a_{2m}\pi_+^{2m}}{(2m!)^{1/2}\epsilon^m}\right)|0\rangle \ . \tag{9}$$

Here, a_6, for example, is a complex parameter which determines the magnitude and phase of the hexagonal distortion of the pair state. In much of this section we will consider only hexagonal distortions.

With $|S\rangle$ taken to be

$$|S\rangle=\left(1+|a_6|^2\right)^{-1/2}\left(1+\frac{a_6\pi_+^6}{\sqrt{6!}\epsilon^3}\right)|0\rangle \tag{10}$$

we find that the expectation value in Eq. (2) can be broken into three separate terms.

$$\langle S|(\vec{v}\cdot\vec{\pi}/2\tilde{\omega})^{2n}|S\rangle=A+|a_6|B+|a_6|^2C \ , \tag{11}$$

where

$$A=\langle 0|(\vec{v}\cdot\vec{\pi}/2\tilde{\omega})^{2n}|0\rangle=a^n(2n-1)!! \ , \tag{12}$$

$$B=\frac{1}{\sqrt{6!}\epsilon^3}\left[\frac{a_6}{|a_6|}\left\langle 0\left|\left(\frac{\vec{v}\cdot\vec{\pi}}{2\tilde{\omega}}\right)^{2n}\pi_+^6\right|0\right\rangle+\text{H.c.}\right]$$

$$=\frac{2\cos(6\phi+\phi_6)}{\sqrt{6!}}a^nP(n) \ , \tag{13}$$

and

$$C=\frac{1}{6!\epsilon^6}\left\langle 0\left|\pi_-^6\left(\frac{\vec{v}\cdot\vec{\pi}}{2\tilde{\omega}}\right)^{2n}\pi_+^6\right|0\right\rangle=(1/6!)a^nQ(n) \ . \tag{14}$$

Here, ϕ_6 is defined by $a_6=|a_6|\exp(i\phi_6)$, and as before, $a=v_1^2eH_{c2}/4\tilde{\omega}^2$. The functions $P(n)$ and $Q(n)$ are found by making repeated use of Eq. (6) and the

commutation relation $[\pi_-, \pi_+] = \epsilon$, and are given by

$$P(n) = \begin{cases} (2n+5)!! - 15(2n+3)!! + 45(2n+1)!! - 15(2n-1)!!, & n \geq 3 \\ 0, \text{ otherwise} \end{cases}, \tag{15}$$

$$Q(n) = (2n+11)!! - 30(2n+9)!! + 315(2n+7)!! - 1380(2n+5)!! + 2475(2n+3)!! - 1350(2n+1)!! + 225(2n-1)!! \; . \tag{16}$$

Each of the sums over n of the terms in Eqs. (12)–(14) is essentially identical to the sum in Eqs. (7) and (8) and can therefore be evaluated exactly. Numerical solutions to Eq. (3) with $|S\rangle$ hexagonally distorted as given by Eq. (10) are shown in Fig. 5. We observe that even small amounts of pair-state anisotropy cause positive curvature in $h^*(t)$ near $t=1$, and increased values of $h^*(t)$ for lower temperatures. Further calculations indicate that as impurity scattering is increased, the effects of pair-state anisotropy vanish in a manner nearly identical to that shown in Fig. 4.

Expression B [Eqs. (11) and (13)] is the coefficient on a term linear in the pair-state anisotropy. By changing the phase of a_6 (i.e., by rotating the pair-state anisotropy relative to the Fermi-surface anisotropy) we can estimate the contribution of this linear term to $h^*(t)$. Numerical results are shown in Fig. 6.

Although the model used by Teichler[11] is quite unlike the model developed here and the approximations he made cannot easily be compared with ours, it is possible to contrast some of his results with ours. First, our $h^*(t)$ curve lies on or above Helfand and Werthamer's[8] curve for $h^*(t)$ in isotropic materials regardless of the relative phase of the Fermi-surface anisotropy and the pair-state anisotropy (Fig. 6). Teichler's $h^*(t)$ curves can fall below Helfand and Werthamer's curves for some reasonable values of his parameters. Secondly, we find that terms linear in the pair-state anisotropy [term B, Eqs. (11) and (13)] contribute significantly to $h^*(t)$ at low temperatures. Teichler's formalism contains no such linear terms. Although parametrized differently, many of our other results are, however, qualitatively similar to Teichler's.

If the crystal symmetry perpendicular to the field is not hexagonal but either ellipsoidal or cubic, the pair state is described by

$$|S\rangle = (1 + |a_2|^2 + |a_4|^2)^{-1/2} \left(1 + \frac{a_2 \pi_+^2}{\sqrt{2!}\epsilon} + \frac{a_4 \pi_+^4}{\sqrt{4!}\epsilon^2}\right)|0\rangle \; . \tag{17}$$

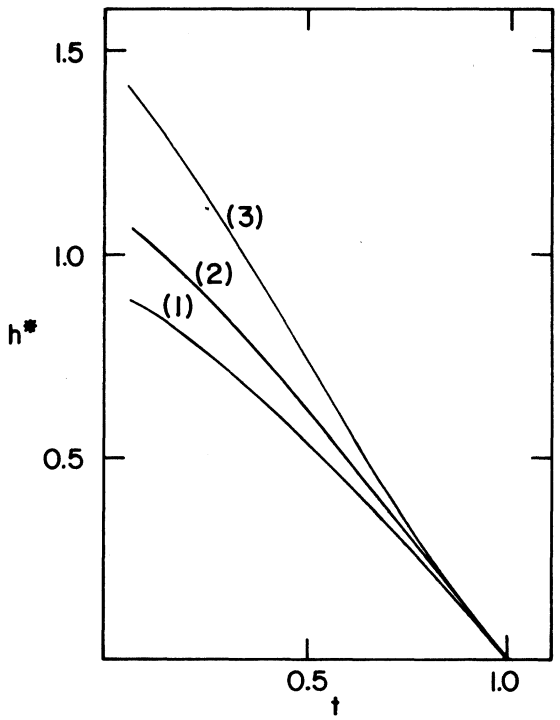

FIG. 5. Upper critical fields for materials with distorted Fermi surfaces and distorted superconducting pair states. $\lambda = 0.0$, $b_6 = 0.4$, $a_6 =$ (1) 0.0; (2) 0.15; (3) 0.3.

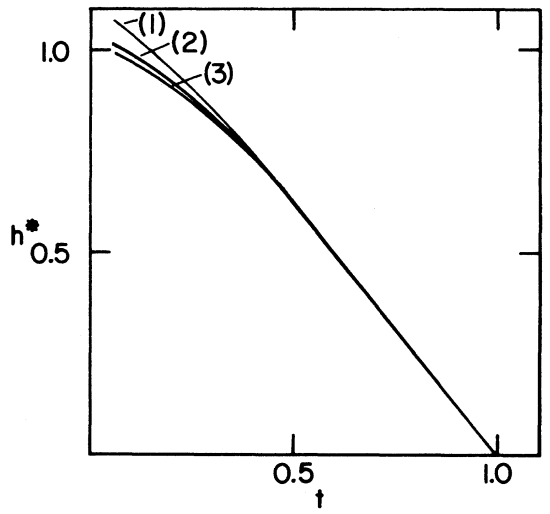

FIG. 6. Upper critical fields. ϕ_6 measures the rotation of the pair-state anisotropy relative to the Fermi-surface anisotropy. $\lambda = 0.0$, $a_6 = 0.15$, $b_6 = 0.4$, $\phi_6 =$ (1) 0.0; (2) $\frac{1}{2}\pi$; (3) π.

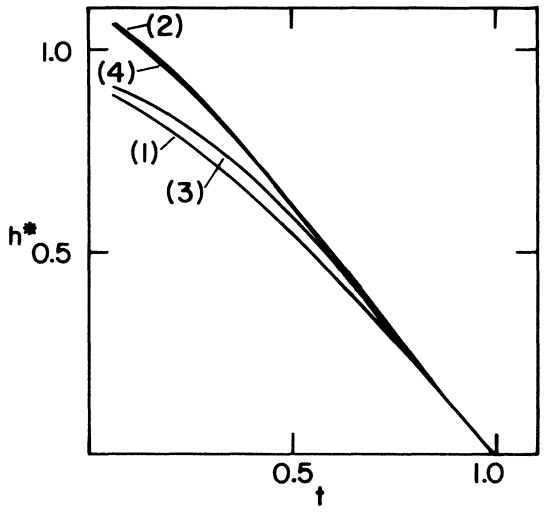

FIG. 7. Upper critical fields for ellipsoidally, cubicly, and hexagonally distorted Fermi surfaces and pair states. $\lambda=0.0$, $\phi_n=0.0$, $a_n=0.0$, $b_n=0.0$ except: (1) $b_n=0.4$ (any n); (2) $a_2=0.15$; $b_2=0.4$; (3) $a_4=0.15$, $b_4=0.4$; (4) $a_6=0.15$; $b_6=0.4$.

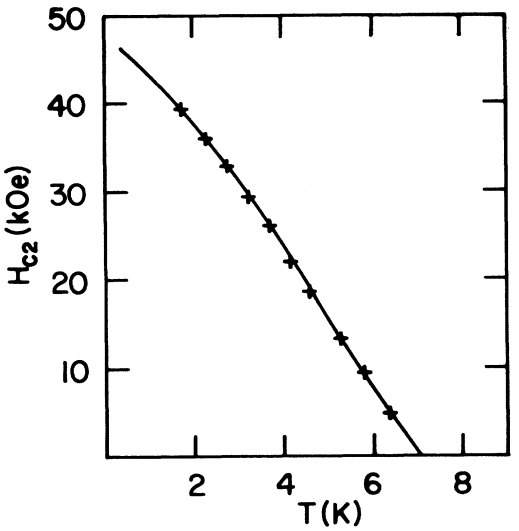

FIG. 8. Fit to experimental $H_{c2\perp}$ data[2] (+) on $2H$-$NbSe_2$. $\lambda=0.0$, $a_6=0.12$, $b_6=0.34$, $\phi_6=0.0$, $T_{c0}=7.06$ K, $\alpha=0.071$.

The sum over n from Eq. (2) can now be broken into six separate sums similar to those in Eqs. (12)–(14) (see Appendix B). Numerical results depicted in Fig. 7 show that ellipsoidal and hexagonal pair-state perturbations cause significantly more enhancement of $h^*(t)$ than do cubic perturbations. The reason for this is not understood.

In Fig. 8 we fit our theory to experimental data[2] on $2H$-$NbSe_2$, a material with hexagonal symmetry in the layers. Here $\alpha \equiv T_{c0}m^*/\epsilon_F m$ is a free parameter which sets the scale of H_{c2}, and m^* is an average effective mass of the conduction electrons. The choice of $b_6=0.34$ is consistent with Fermi-surface calculations done by Wexler and Woolley.[15] Prober *et al.*[16] estimate $\lambda \approx \xi_0/l=0.15$ for $NbSe_2$. If we were to fit the data with $\lambda \neq 0$, b_6 and a_6 would be slightly larger and α would be slightly smaller.

ACKNOWLEDGMENTS

This work was supported by the U.S. DOE, Contract No. W-7405-Eng-82, Division of Materials Sciences, Budget Code AK-01-02-02-3. We are indebted to D. E. Prober, K. Machida, J. Berlinsky, and T. M. Rice for many valuable discussions, and to D. E. Prober, B. J. Dalrymple, and T. P. Orlando for sending us their results prior to publication.

APPENDIX A

If $\lambda=0$ and the Fermi surface is spherically symmetric so $N(\hat{q})=1/4\pi$ and

$$\int d\hat{q}N(\hat{q})v_1^{2n}=v_F^{2n}\frac{2^n n!}{(2n+1)!!} , \tag{18}$$

Eqs. (2), (3), and (7) become

$$\ln\left(\frac{T}{T_{c0}}\right)=\sum_{\nu=-\infty}^{\infty}\frac{\pi T}{|\omega|}\sum_{n=1}^{\infty}(-1)^n\left(\frac{eH_{c2}v_F^2}{4\omega^2}\right)^n\frac{2^n n!}{(2n+1)!!}(2n-1)!! \tag{19}$$

or

$$\ln t=\sum_{\nu=-\infty}^{\infty}\left[\frac{1}{|2\nu+1|}-\frac{1}{|2\nu+1|}\sum_{n=0}^{\infty}(-1)^n\left(\frac{(2h)^{1/2}}{t(2\nu+1)}\right)^{2n}\frac{n!}{2n+1}\right] , \tag{20}$$

where t and h are defined in Sec. III. Our Eq. (20) is identical to Eqs. (24) and (36) in Ref. 8.

APPENDIX B

With $|S\rangle$ described by Eq. (17) we find

$$\langle S|(\vec{v}\cdot\vec{\pi}/2\tilde{\omega})^{2n}|S\rangle = A + |a_2|D + |a_2|^2E + |a_4|F + |a_2||a_4|G + |a_4|^2H \ , \tag{21}$$

where A is given by Eq. (12),

$$D = \frac{1}{\sqrt{2!}\epsilon}\left[\frac{a_2}{|a_2|}\left\langle 0\left|\left(\frac{\vec{v}\cdot\vec{\pi}}{2\tilde{\omega}}\right)^{2n}\pi_+^2\right|0\right\rangle + \text{H.c.}\right] = \frac{2\cos(2\phi+\phi_2)}{\sqrt{2!}}a^n[(2n+1)!! - (2n-1)!!] \ , \tag{22}$$

$$E = \frac{1}{2!\epsilon^2}\left\langle 0\left|\pi_-^2\left(\frac{\vec{v}\cdot\vec{\pi}}{2\tilde{\omega}}\right)^{2n}\pi_+^2\right|0\right\rangle = (1/2!)a^n[(2n+3)!! - 2(2n+1)!! + (2n-1)!!] \ , \tag{23}$$

$$F = \frac{1}{\sqrt{4!}\epsilon^2}\left[\frac{a_4}{|a_4|}\left\langle 0\left|\left(\frac{\vec{v}\cdot\vec{\pi}}{2\tilde{\omega}}\right)^{2n}\pi_+^4\right|0\right\rangle + \text{H.c.}\right] = \frac{2\cos(4\phi+\phi_4)}{\sqrt{4!}}a^n[(2n+3)!! - 6(2n+1)!! + 3(2n-1)!!] \ , \tag{24}$$

$$G = \frac{1}{(2!4!)^{1/2}\epsilon^3}\left[\frac{a_2^* a_4}{|a_2||a_4|}\left\langle 0\left|\pi_-^2\left(\frac{\vec{v}\cdot\vec{\pi}}{2\tilde{\omega}}\right)^{2n}\pi_+^4\right|0\right\rangle + \text{H.c.}\right] = \frac{2\cos(2\phi+\phi_4-\phi_2)}{(2!4!)^{1/2}}a^n[(2n+5)!! - 7(2n+3)!! + 9(2n+1) - 3(2n-1)!!] \ , \tag{25}$$

$$H = \frac{1}{4!\epsilon^4}\left\langle 0\left|\pi_-^4\left(\frac{\vec{v}\cdot\vec{\pi}}{2\tilde{\omega}}\right)^{2n}\pi_+^4\right|0\right\rangle = (a^n/4!)[(2n+7)!! - 12(2n+5)!! + 42(2n+3)!! - 36(2n+1)!! + 9(2n-1)!!] \tag{26}$$

Here, ϕ_2 and ϕ_4 are defined by $a_2 = |a_2|\exp(i\phi_2)$ and $a_4 = |a_4|\exp(i\phi_4)$.

[1]T. P. Orlando, E. J. McNiff, Jr., S. Foner, and M. R. Beasley, Phys. Rev. B 19, 4545 (1979), and (private communication).

[2]B. J. Dalrymple and D. E. Prober, Bull. Am. Phys. Soc. 23, 230 (1978), and (private communication).

[3]N. Toyota, H. Nakatsuji, K. Nota, A. Hoshi, N. Kobayashi, and Y. Muto, J. Low Temp. Phys. 25, 483 (1976).

[4]S. Foner and E. J. McNiff, Jr., Phys. Lett. A 45, 429 (1973).

[5]J. A. Woollam, R. B. Somoano, and P. O'Connor, Phys. Rev. Lett. 32, 712 (1974).

[6]H. W. Weber, E. Seidl, and G. Kirschenhofer, Solid State Commun. 26, 795 (1978).

[7]T. Ohtsuka, in *Anisotropy Effects in Superconductors*, edited by H. W. Weber (Plenum, New York, 1977), pp. 27–41.

[8]E. Helfand and N. R. Werthamer, Phys. Rev. 147, 288 (1966).

[9]P. C. Hohenberg and N. R. Werthamer, Phys. Rev. 153, 493 (1967).

[10]K. Takanaka and T. Nagashima, Prog. Theor. Phys. 43, 18 (1970).

[11]H. Teichler, Phys. Status Solidi 72, 211 (1975).

[12]Landau quantization which becomes important when $eH_{c2}/m \approx \pi T + 1/\tau$ is not considered in this paper.

[13]A. A. Maradudin, E. W. Montroll, and G. H. Weiss, *Theory of Lattice Dynamics in the Harmonic Approximation* (Academic, New York, 1963), Chap. VII, Sec. 2.

[14]Hohenberg and Werthamer (Ref. 9) kept the first three terms in this series. Takanaka and Nagashima (Ref. 10) kept the first four terms.

[15]G. Wexler and A. M. Woolley, J. Phys. C 9, 1185 (1976).

[16]D. E. Prober, R. E. Schwall, and M. R. Beasley (unpublished).